

A HIGH-SENSITIVE SUZAKU OBSERVATION OF POSSIBLE NON-THERMAL EMISSION FROM A WHITE DWARF

Y. Terada¹, M. Ishida², K. Mukai³, K. Makishima^{1,4}, T. Dotani⁵, L. Gallo⁵, S. Naik⁵, T. Hayashi⁵, S. Okada⁵, R. Nakamura⁵, and T. Enoto⁴

¹RIKEN, 2-1 Hirosawa Wako, Saitama, Japan

²Tokyo Metropolitan University, 1-1 Minami-Osawa Hachioji, Tokyo, Japan

³NASA/GSFC, Code 660 Greenbelt MD 20771, USA

⁴Univ. of Tokyo, 7-3-1 Hongo Bunkyo-ku, Tokyo, Japan

⁵ISAS/JAXA, 3-1-1 Yoshinodai Sagami-hara, Kanagawa, Japan

ABSTRACT

As system similar to a rotating neutron star, a strongly magnetized white dwarf (WD) may be a moderate particle acceleration site. At the best case, the induced electric field is expected to reach 10^{13} to 10^{14} eV. A trial to detect non-thermal emission from a best candidate among WDs, AE Aquarii, was performed with the hard X-ray detector (HXD) on-board the fifth Japanese X-ray satellite, Suzaku. Although the HXD has a non-imaging capability, the sensitivity in the 10 – 70 keV band reaches about the 5×10^{-6} – 10^{-5} photons/sec/cm²/keV level with only 100 msec exposure. Marginal detection has been achieved with the HXD, which was separated from the thermal emission. If this is real, it must be the first case of a detection of non-thermal emission from WDs.

Key words: acceleration of particles – stars: white dwarfs – X-rays: individual (AE Aquarii).

1. MAGNETIZED WHITE DWARFS AS PARTICLE ACCELERATION SITES

According to Hillas[18] or Makishima [24], the maximum particle energy, E_{\max} , observed in various particle-acceleration sites, including the rotating neutron stars (NSs), as well as aurora sub-storms, solar flares, blazar jets, shell-like and Crab-like supernova remnants) generally scales as

$$E_{\max} \sim e v B L, \quad (1)$$

where e is the elementary charge, B the magnetic strength, and L the typical scale of objects. Among these astrophysical objects, rotating NSs have been regarded to be a textbook case of particle-acceleration sites, though details of the acceleration mechanism are not very well understood (for example, the “polar cap” model or the “outer gap” model). To solve the model degeneracy, it is useful to study similar systems with very different physical parameters. In a Hillas diagram, we can expect non-

thermal emission from magnetized white dwarfs (WDs), in addition to cluster of galaxies. Strong magnetized WDs are ideal for this purpose, because they have essentially the same system geometry as NSs, but differ greatly from NSs regarding the system parameters of e , B , and L . The induced electric fields from strongly magnetized WDs are expected to reach 10^{13} to 10^{14} eV, as shown in figure 1.

With several searches in the radio band [31, 8, 32], non-thermal incoherent emission has actually been detected from five WDs. Some objects, like AE Aqr [4] and AM Her [13, 15], show signs of coherent radio emission. In addition, the last two objects are reported to show TeV gamma-ray emission during optical flares (AE Aqr:[10, 28, 29] and AM Her [9]). Therefore, high-energy electrons with about 1-100 MeV energies do exist in WDs [3, 5]. In this situation, high energy photons in the X-ray band must be generated via a “non-thermal” mechanism. Hard X-ray emission, itself, has been reported by the INTEGRAL IBIS survey from 19 objects[6]. This paper deals with a highly sensitive search for a “non-thermal” component from a most likely object, AE Aquarii, with *Suzaku*.

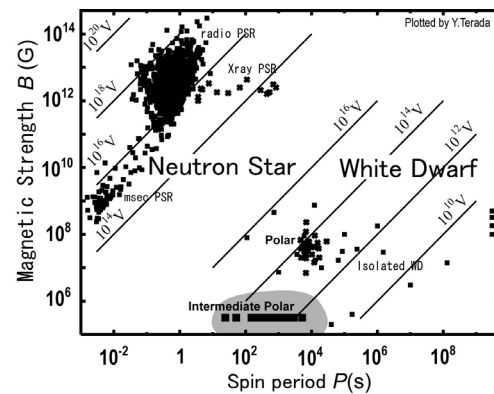


Figure 1. Scatter plot of P versus B for NSs and WDs. The lines show the induced electric potential for NSs and WDs, respectively. (NSs data [25, 24]; WDs [39, 34, 35])

2. HIGH SENSITIVE SEARCH WITH SUZAKU

2.1. Most likely object, AE Aquarii

Among cataclysmic variables of WD binaries, AM Hercuris (Polar), and AE Aquarii (Intermediate Polar) have the maximum induced potential of over 10^{14} eV, as can be seen in figure 1. Between two objects, AE Aquarii has the advantages listed below from the viewpoint of a non-thermal emitter [37].

- Radio synchrotron flares have been reported by many authors [7, 1, 4, 2, 3, 5]. They are consistent with 2000 G synchrotron emission [27].
- Pulsed TeV gamma-rays have been observed [11, 28, 29], which are sometimes synchronized with optical flares.
- The WD is rotating while being close to the break-up condition. It has the second fastest spinning period of ~ 33.0767 sec among the MCVs, and is the most asynchronous binary with an orbital period of 9.88 hr [12].
- The accreting matter may be inhibited from reaching the WD surface by fast WD rotation. The plasma temperature measured in X-ray bremsstrahlung is abnormally lower than the gravitational potential of WD [17, 19], and the UV to X-ray luminosity (10^{31} erg s^{-1}) is three orders of magnitude lower than that in a simple accretion case ([14, 16]) with a rate of 10^{17} g s^{-1} .
- A magnetic propeller effect occurs in the system. Only 1% of the gas emits UV photons, and almost all of it is are propellered out [40].
- It is a spin down object at a rate of 1.8×10^{-6} s yr^{-1} [41], in contrast to the general spin-up trend among MCVs. The value corresponds to a huge spin-down luminosity of 5×10^{33} erg s^{-1} .

2.2. The Hard X-ray Detector onboard Suzaku

In searching for possible non-thermal emission from WDs, it is difficult to conduct high-sensitivity spectroscopy in the hard X-ray to soft gamma-ray energy bandpass, where the Compton-scattering process becomes dominant, rather than the photoelectric absorption process. Furthermore, the source intensity is usually weaker than the detector background at these energies, so that the sensitivity is mainly limited by the background level. In orbit, background events arise due to diffuse gamma-ray emission, non X-ray events caused directly by primary and secondary cosmic-rays, and radio-activated nuclei inside the detector, induced by MeV protons trapped in a low Earth orbit.

The Hard X-ray Detector (HXD) onboard *Suzaku* is an instrument which is designed particularly to archive a sufficiently low background level [20, 21, 36]. The spacecraft, *Suzaku*, is the fifth in a series of Japanese X-ray satellites [30] in collaboration with Japan and US, and is a recovery mission of *Astro-E*, which was lost in launching failure in 2000. *Suzaku* was successfully launched on 10 July, 2005 from Uchinoura Space Center in Japan with the Japanese solid-fuel vehicle of the M-V rocket. In addition to the HXD, which covers 10–70 keV with PIN diodes and 40–600 keV with $Gd_2SiO_5:Ce$ (GSO) scintillators [33, 22], it carries onboard the X-ray Imaging Spectrometer (XIS), operating at 0.2–12 keV [26, 23].

The main photo-absorbing materials of the HXD sensor are PIN diodes and GSO crystals, which are installed at the bottom inside of a well-shaped BGO shield crystal, as shown in figure 2. The most important feature of the HXD sensor is the narrow field-of-view (FOV) of 0.57° and 4.5° square for PINs and GSOs, respectively. In other words, the importance is completeness of the active shielding configuration by many BGO crystals. It enables us to reduce not only non-X-ray backgrounds of particle events by anti-coincidence methods between units, but also Comptonized X-ray events by a pulse-shaped discrimination technique [33].

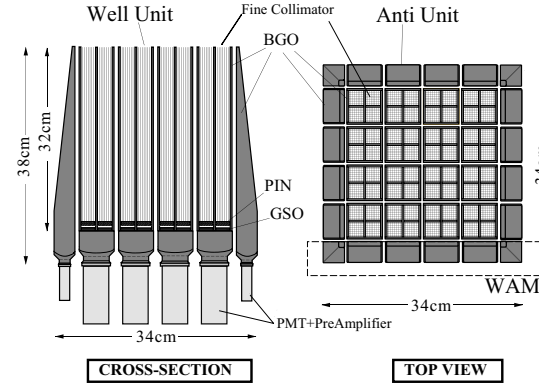


Figure 2. Schematic view of the Hard X-ray Detector onboard *Suzaku*. The HXD sensor consists of 16 identical GSO/BGO well-type-phoswich counters, incorporating 2 mm-thick silicon PIN diodes, and surrounding 20 BGO shield counters.

2.3. Observation with Suzaku

We observed AE Aquarii with *Suzaku* from 2:13UT on 2005 October 30 to 01:02UT on 2005 November 2. The observation was carried out at the “HXD nominal” pointing position (i.e., putting the target at the optical axis of the HXD), for a net exposure of 47.0 ksec with the XIS and 52.7 ksec with the HXD. The XIS was operated in the normal mode with “1/8 window” option, which gave a time resolution of 1 sec, whereas the HXD was in the nominal mode. In October 2006, we observed AE Aquarii again with 40 ksec, and further analyses combined with two observations will be reported in a future paper [38].

3. ANALYSIS AND RESULTS

3.1. Signal detection by PIN diodes

We used the dataset of version 1.2.2.3 comparable products. In an analysis of the HXD data, we excluded all of the telemetry-saturated data, and data taken in the “low” rate acquisition mode, and removed events in time intervals when the source elevation above the earth’s limb was below 5° , or the spacecraft was in and up-to-436 sec after the South Atlantic Anomaly (SAA), and when the geomagnetic cutoff rigidity was lower than 8 GV. After this filtering, the final HXD event list was obtained after standard anti-coincidence selection of the HXD [33].

The non X-ray background (NXB) of the PIN diodes was synthesized by appropriately combining night-earth data sets acquired under different conditions [22]. We checked the reliability of NXB estimation of this observation by comparing real data and simulated NXB data while the spacecraft observed the Earth, as shown in figure 3. The net exposure of the Earth’s events leave 43.0 ksec, and the difference was about 1% in 10 – 50 keV band for this observation.

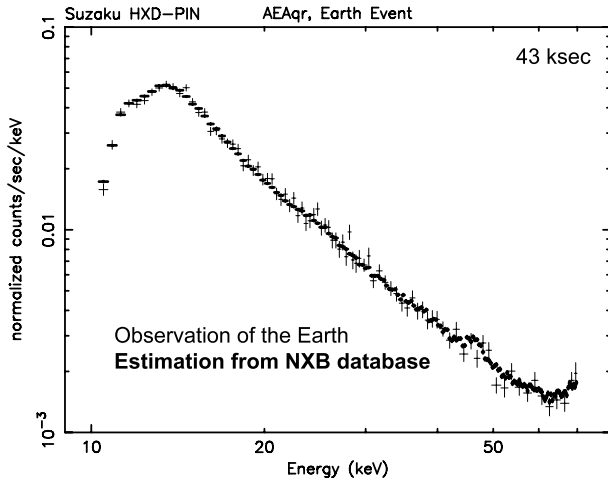


Figure 3. Comparison of X-ray spectra of real data and estimated NXB, when the spacecraft observed the Earth.

We then extracted the PIN spectra as shown in figure 4. The signals were clearly detected below 30 keV, when the systematics of NXB estimation was about 3%. It is almost consistent with the Cosmic X-ray background events coming into $0.57^\circ \times 0.57^\circ$ FOV of PINs.

3.2. PIN detections free from systematics: Timing

The PIN spectrum in figure 4 includes a few % level of systematic errors in the estimation and modeling of NXB and the CXB spectra, which is comparable with the signal, if it exists. Thus, we performed a phase-resolved spectroscopy with the rotation period of the WD, and

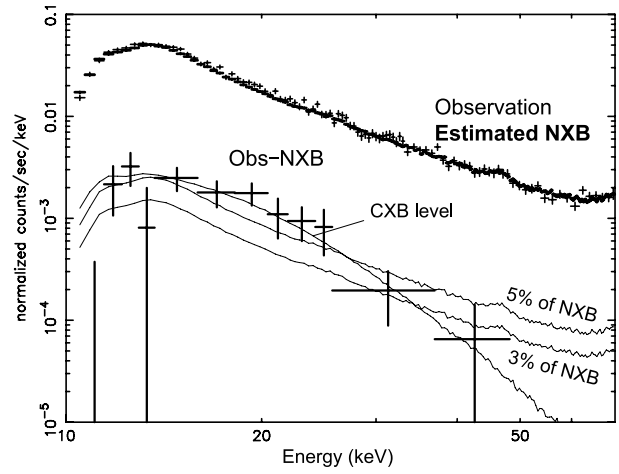


Figure 4. X-ray spectra of AE Aqrarii with HXD PIN diodes. Thin and thick plots are observed data and estimated NXB, respectively. The difference is also plotted. Thin lines show 3 and 5% of NXB, and the CXB.

made an on–off spectrum. It is free from any systematics in the NXB estimation if the timescale of the variability of the NXB is larger than the source period of 33 sec, and CXB emission in the spectrum is canceled out.

The source pulsations were detected at a barycentric period of 33.07975 ± 0.00002 sec over the full XIS band, and modulations are clearly seen in the folded light curves (figure 5 top). We found a shallow modulation in the HXD data in 10 – 25 keV band with the best period by the XIS, as shown in figure 5, bottom, although it is consistent with constant. We then extracted the X-ray spectra of pulsation components by subtracting the spectra in the maximum phase (hatched in figure 5) by those in the minimum phase, as shown in figure 6 left. We found marginal signals in the 10 – 20 keV band with PIN diodes.

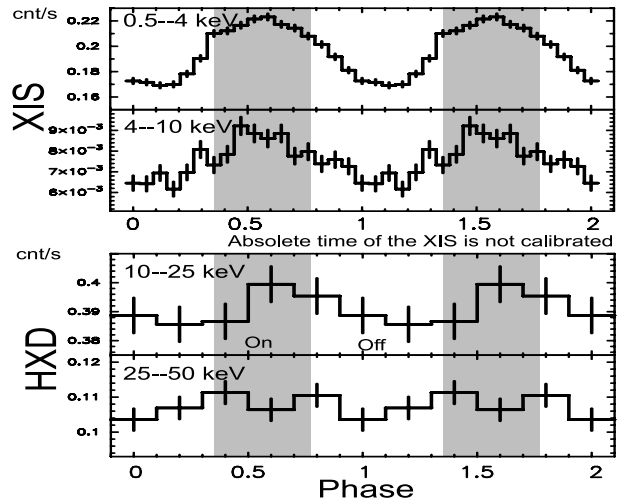


Figure 5. Energy resolved light curves folded with the period of 33.07975 sec, obtained by the XIS.

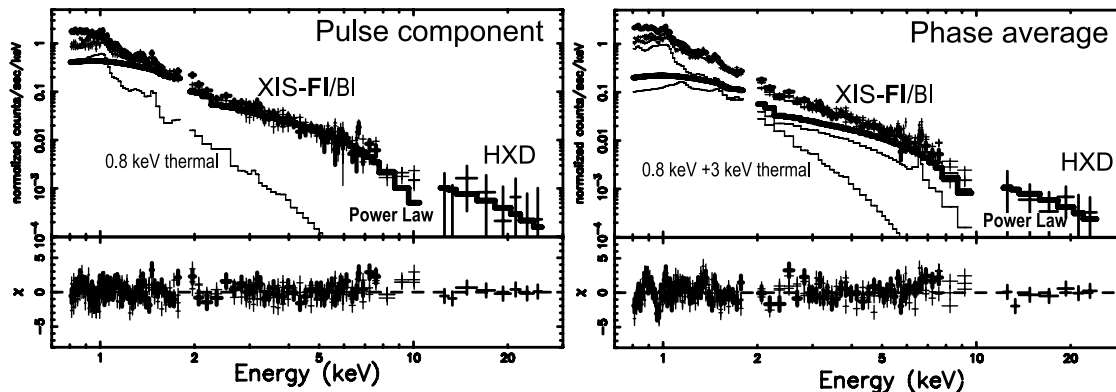


Figure 6. Left: X-ray spectra of AE Aqr of pulsation component (see the text). Right: Phase averaged spectra. Data are shown in crosses, and thin and thick lines are best fit models (see the text).

3.3. Wide-band X-ray Spectra of AE Aquarii

We extracted spectra of the XIS within $4'.3$ of the image centroid after standard screening [23], and subtracted any background spectra reproduced by combining a night Earth database.

The wide-band spectra of pulse component (figure 6 left) were well reproduced by a simple power-law model in the 3 – 25 keV band, with a photon index of 2.29 ± 0.04 and a flux of $(3.5 \pm 0.2) \times 10^{-12}$ ergs s^{-1} cm^{-2} at 10 – 100 keV. If we expand the lower energy into 0.8 keV, the spectra require additional thermal component with a temperature of 0.87 ± 0.01 keV in the Raymond Smith model. As for the minimum phase, the spectra does not require a non-thermal component, but requires another thermal component with a temperature of $3.12^{+0.19}_{-0.12}$ keV, in addition to the original 0.83 ± 0.05 keV component with an abundance of 0.27 ± 0.04 solar. We could then reproduce the phase-averaged X-ray spectra (figure 6 right) by the following components:

1. stable 3.12 keV thermal component,
2. variable 0.84 ± 0.01 keV thermal component,
3. variable non-thermal emission with index of $2.10^{+0.05}_{-0.20}$ and flux $(4.1 \pm 1.1) \times 10^{-12}$ erg s^{-1} cm^{-2} , (which appears only in maximum phase).

In summary, if this picture is correct, the flux of the non-thermal radiation from the WD is no larger than 0.1% of the spin-down energy.

ACKNOWLEDGMENTS

The authors would like to thank all the members of the *Suzaku* Science Working Group for their many tasks.

REFERENCES

[1] Abada-Simon, M., *et al.* 1993, ApJ, 406, 692
 [2] Abada-Simon, M., *et al.* 1995a, ASP, 85, 355
 [3] Abada-Simon, M., *et al.* 1999, ESA-SP, 427
 [4] Abada-Simon, M., *et al.* 1996, ASP Con, 93, 182

[5] Abada-Simon, M., *et al.* 2002, SF2A, EdP-Sci, C.497
 [6] Barlow, E. J. *et al.* 2006 MNRAS, 372, 224
 [7] Bastian *et al.* 1988, ApJ, 324, 431
 [8] Beasley *et al.* 1994 AJ 108, 2207
 [9] Bhat *et al.* 1991, ApJ, 369, 475
 [10] Bowden *et al.* 1991, Proc 22d Int. CR Conf. 1, 356
 [11] Brink *et al.* 1990, Proc 22d Int. CR Conf. 2, 283
 [12] Casares *et al.* 1996 MNRAS 282, 182
 [13] Chanmugam G., and Dulk G. A. 1982, ApJ 255, 107
 [14] Dhillon, 1996, CVs and Related Objects. Kluwer, p3
 [15] Dulk G.A. *et al.* 1983, ApJ 273, 249
 [16] Eracleous and Horne, 1996, ApJ, 471, 427
 [17] Ezuka and Ishida M., 1999, ApJS, 120, 277
 [18] Hillas A. M. 1984, ARA&A 22, 425
 [19] Itoh K. *et al.* ApJ 639, 397
 [20] Kawaharada M. *et al.* 2004, SPIE, 5501, 286
 [21] Kokubun M. *et al.* 2004, IEEE TNS 51 5, 1991
 [22] Kokubun M. *et al.* 2007, PASJ 59, S35
 [23] Koyama K. *et al.* 2007, PASJ 59, S9
 [24] Makishima K., *et al.* 1999, ApJ, 525, 978
 [25] Manchester R. N. *et al.* 2001, MNRAS, 328, 17-35
 [26] Matsumoto H. *et al.* 2005, NIM A, 541, 357
 [27] Meintjes and Venter 2003, MNRAS 341, 891
 [28] Meintjes *et al.* 1992, ApJ, 401, 325
 [29] Meintjes *et al.* 1994, ApJ 434, 292
 [30] Mitsuda K. *et al.* 2007, PASJ 59, S1
 [31] Nelson R. F. *et al.* 1988 MNRAS 234, 1105
 [32] Pavelin P. E., *et al.* 1994, MNRAS 269, 779
 [33] Takahashi T. *et al.* 2007, PASJ 59, S35
 [34] Terada Y. *et al.* 2001, MNRAS 328, 112
 [35] Terada Y. *et al.* 2004, PASJ 56, 533
 [36] Terada Y. *et al.* 2005, IEEE TNS 52 4, 902
 [37] Terada Y. *et al.* 2007, JASR in prep.
 [38] Terada Y. *et al.* 2007, PASJ 59 to be submitted
 [39] Wickramasinghe D. T. *et al.* 2000, PASP 112, 873
 [40] Wynn *et al.* 1997, MNRAS 286, 436
 [41] de Jager *et al.* 1994, ApJ, 90, 775